JCI The Journal of Clinical Investigation

Molecular basis for the modulation of native T-type Ca^{2+} channels in vivo by Ca^{2+} /calmodulin-dependent protein kinase II

Junlan Yao, … , Roger J. Colbran, Paula Q. Barrett

J Clin Invest. 2006;116(9):2403-2412. https://doi.org/10.1172/JCI27918.

Research Article **Cardiology**

Ang II receptor activation increases cytosolic Ca^{2+} levels to enhance the synthesis and secretion of aldosterone, a recently identified early pathogenic stimulus that adversely influences cardiovascular homeostasis. Ca^{2+}/calmodulin-dependent protein kinase II (CaMKII) is a downstream effector of the Ang II–elicited signaling cascade that serves as a key intracellular Ca^{2+} sensor to feedback-regulate Ca^{2+} entry through voltage-gated Ca^{2+} channels. However, the molecular mechanism(s) by which CaMKII regulates these important physiological targets to increase Ca^{2+} entry remain unresolved. We show here that CaMKII forms a signaling complex with α_{1H} T-type Ca^{2+} channels, directly interacting with the intracellular loop connecting domains II and III of the channel pore (II-III loop). Activation of the kinase mediated the phosphorylation of Ser1198 in the II-III loop and the positive feedback regulation of channel gating both in intact cells in situ and in cells of the native adrenal zona glomerulosa stimulated by Ang II in vivo. These data define the molecular basis for the in vivo modulation of native T-type Ca^{2+} channels by CaMKII and suggest that the disruption of this signaling complex in the zona glomerulosa may provide a new therapeutic approach to limit aldosterone production and cardiovascular disease progression.

Molecular basis for the modulation of native T-type Ca^{2+} channels in vivo by Ca^{2+}/calmodulin-dependent protein kinase II

Junlan Yao,[1] Lucinda A. Davies,[1] Jason D. Howard,[1] Scott K. Adney,[1] Philip J. Welsby,[1] Nancy Howell,[2] Robert M. Carey,[2] Roger J. Colbran,[3] and Paula Q. Barrett[1]

[1]Department of Pharmacology and [2]Department of Medicine, University of Virginia School of Medicine, Charlottesville, Virginia, USA.
[3]Department of Molecular Physiology and Biophysics, Vanderbilt University School of Medicine, Nashville, Tennessee, USA.

Ang II receptor activation increases cytosolic Ca^{2+} levels to enhance the synthesis and secretion of aldosterone, a recently identified early pathogenic stimulus that adversely influences cardiovascular homeostasis. Ca^{2+}/calmodulin-dependent protein kinase II (CaMKII) is a downstream effector of the Ang II–elicited signaling cascade that serves as a key intracellular Ca^{2+} sensor to feedback-regulate Ca^{2+} entry through voltage-gated Ca^{2+} channels. However, the molecular mechanism(s) by which CaMKII regulates these important physiological targets to increase Ca^{2+} entry remain unresolved. We show here that CaMKII forms a signaling complex with α_{1H} T-type Ca^{2+} channels, directly interacting with the intracellular loop connecting domains II and III of the channel pore (II-III loop). Activation of the kinase mediated the phosphorylation of Ser1198 in the II-III loop and the positive feedback regulation of channel gating both in intact cells in situ and in cells of the native adrenal zona glomerulosa stimulated by Ang II in vivo. These data define the molecular basis for the in vivo modulation of native T-type Ca^{2+} channels by CaMKII and suggest that the disruption of this signaling complex in the zona glomerulosa may provide a new therapeutic approach to limit aldosterone production and cardiovascular disease progression.

Introduction

Abnormal intracellular Ca^{2+} homeostasis is a common feature of cardiovascular disease (1, 2). In the human failing heart, arrhythmogenic remodeling is characterized by dysregulated sarcoplasmic reticulum Ca^{2+} uptake and release, enhanced Na-Ca^{2+} exchange activity, and increased activity of L-type high voltage–activated (HVA) Ca^{2+} channels (α_{1C}) (3–5) in cardiomyocytes. Central to these pathologies is an increase in adrenergic tone and a marked activation of the renin-angiotensin aldosterone axis. The importance of aldosterone as an early-onset pathogenic stimulus has been highlighted by recent findings. Following myocardial infarction, inappropriate mineralocorticoid receptor activation increases L-type Ca^{2+} channel density before the onset of structural hypertrophy (6), and chronic levels of circulating aldosterone correlate directly with the density of L-type HVA Ca^{2+} channels in ventricular myocytes that are devoid of morphological change (7). In addition, in the setting of high Na^+ intake, the progression to left-ventricular hypertrophy and failure is advanced by an elevation in aldosterone levels that stimulates perivascular fibrosis (8–10). Thus, long recognized to regulate Na^+ and K^+ balance, blood volume, and blood pressure, aldosterone has a newly appreciated adverse influence on cardiovascular homeostasis.

Aldosterone is synthesized and secreted from the adrenal zona glomerulosa (ZG) cell principally in response to Ang II, ACTH, and physiological increases in extracellular potassium (11). These secretagogues depolarize the ZG cell and/or potentiate Ca^{2+} channel activity (12). Aldosterone production is Ca^{2+} dependent, and low voltage–activated (LVA), T-type Ca^{2+} channels provide the Ca^{2+} that is necessary to sustain its stimulated production (13–15).

Voltage-dependent Ca^{2+} channels change electrical signals into biochemical events. But, because this conversion is adjustable, via changes in channel activity and density, Ca^{2+} channels also can exert additional controls on Ca^{2+}-dependent cellular processes. In the heart, L-type Ca^{2+} channels use Ca^{2+}/calmodulin-dependent protein kinase II (CaMKII) to adjust signal transmission by inducing a gating change that is characterized by frequent channel openings (16). CaMKII expression is increased in structural heart disease (17), and inhibition of its activity reduces Ca^{2+} current and ameliorates dysfunction (18). In the ZG cell, CaMKII induces a gating shift of α_{1H} T-type Ca^{2+} channels that enables more channels to open at hyperpolarized potentials, enhancing Ca^{2+} entry and thus stimulating aldosterone production (19). Although CaMKII regulates both α_{1C} HVA (16, 20, 21) and α_{1H} LVA channels (19, 22, 23), the molecular basis for these effects in vitro and in vivo remains unresolved. Here we analyzed the interaction of CaMKII with α_{1H} T-type Ca^{2+} channels. Our data show that α_{1H} channels use tethered CaMKII as a Ca^{2+} sensor to dynamically regulate channel activity. Moreover, our data indicate that α_{1H} channels are regulated robustly by protein phosphorylation in situ and in vivo, identifying these channels for the first time to our knowledge as authentic physiological targets of kinse activity.

Results

LVA channels are encoded by 3 separate genes: α_{1G}, α_{1H}, and α_{1I}, belonging to the $Ca_v3.0$ family of voltage-gated Ca^{2+} channels (24). CaMKII activation increases whole-cell and single-channel currents mediated by α_{1H} channels by inducing an approximately 12-mV

Nonstandard abbreviations used: $[Ca^{2+}]_i$, intracellular $[Ca^{2+}]$; CaM, calmodulin; CaMKII, Ca^{2+}/calmodulin-dependent protein kinase II; D5W, 5% dextrose; GST, glutathione-S-transferase; HVA, high voltage–activated; LVA, low voltage–activated; PFA, paraformaldehyde; ROI, region of interest; ZG, zona glomerulosa.

Conflict of interest: The authors have declared that no conflict of interest exists.

Citation for this article: *J. Clin. Invest.* **116**:2403–2412 (2006). doi:10.1172/JCI27918.

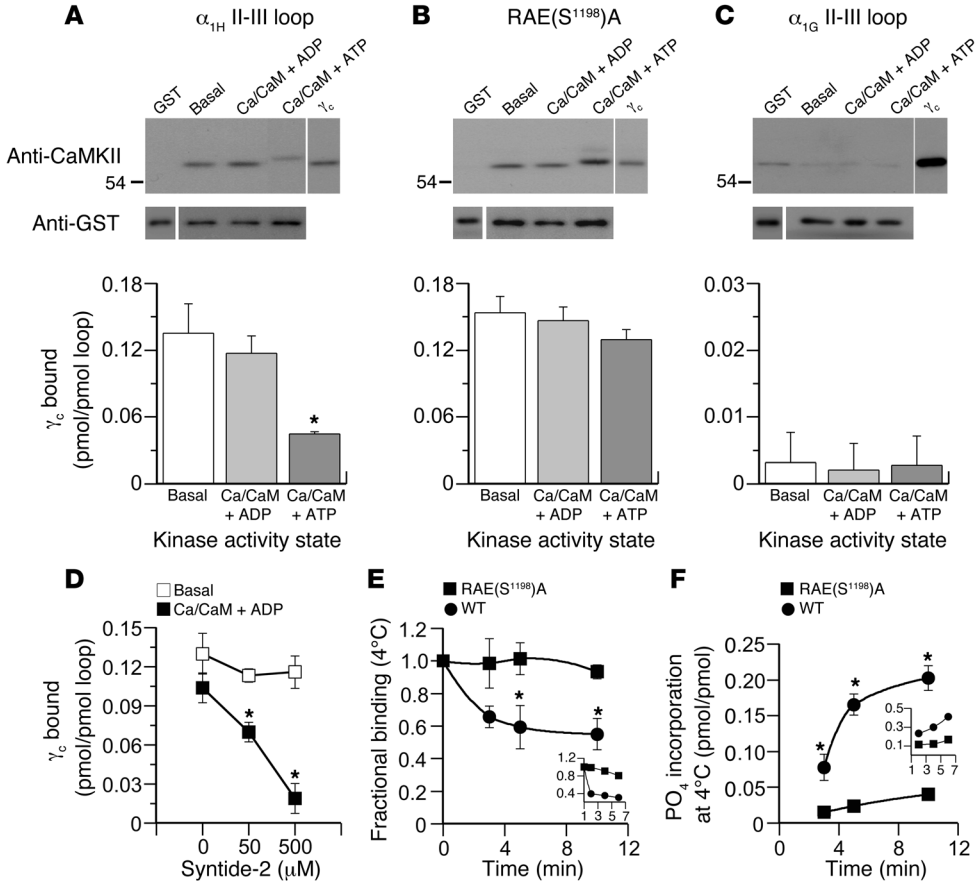

Figure 1

CaMKIIγ_C binds to the α_{1H} II-III loop and is released by loop phosphorylation. (**A**–**C**) Binding of purified recombinant CaMKIIγ_C (5 pmol/250 μl) to bead-bound GST-(II-III) loop fusion proteins (2 pmol). Wild-type α_{1H} II-III loop (**A**), RAE(S1198)A–α_{1H} II-III loop (**B**), or α_{1G} II-III loop (**C**) under autoinhibited (basal), activated (Ca^{2+}/CaM + ADP), or autophosphorylated (Ca^{2+}/CaM + ATP) conditions. Upper panels: immunoblots of bound kinase detected by anti-CaMKII antibody; 0.25 pmol standard for comparison. Equal fusion loading was verified independently in parallel runs (see Methods), and anti-GST detection is shown below. Histograms: quantified mean binding data ± SEM for 5 studies. *$P < 0.05$, Ca^{2+}/CaM + ATP versus basal and Ca^{2+}/CaM + ADP (Kruskal-Wallis ANOVA on Ranks, Dunn's method). (**D**) Competition for autoinhibited or Ca^{2+}/CaM + ADP–activated CaMKII/α_{1H} II-III loop by syntide-2. *$P < 0.05$ (ANOVA, Student-Newman-Keuls method). (**E** and **F**) Time course of 4°C CaMKIIγ_C dissociation and loop phosphorylation following activation of autoinhibited CaMKIIγ_C prebound to GST–α_{1H} II-III loop fusion proteins [wild type vs. RAE(S1198)A]. Activators, Ca^{2+}/CaM + ATP (0.5 mM/5 μM + 0.5 mM), added at $t = 0$. (**E**) Activated-kinase binding determined from quantified immunoblots expressed relative to preactivation values. (**F**) Phosphorylation stoichiometry of GST–α_{1H} II-III loop fusions determined from ^{32}P incorporation. *$P < 0.05$, wild type binding at 5 or 10 minutes versus 0 minutes (ANOVA, Student-Newman-Keuls method). Inset: 30°C. Data are expressed as mean ± SEM ($n = 3$).

hyperpolarizing shift in the half-activation potential for channel opening. This change in activation gating mediated by CaMKII depends on the intracellular loop (residues 1019–1293) connecting channel transmembrane domains II and III and can be abrogated by a Ser1198-to-Ala point mutation (23). Therefore, to characterize the interaction of CaMKII with α_{1H} channels, we began by investigating the binding of purified recombinant CaMKII to the II-III loop, which was expressed as a bacterial fusion protein (see Methods). After the proteins were mixed (8 hours, 4°C), bound kinase was separated using glutathione-sepharose. Binding was quantified against purified recombinant CaMKII protein standards (0.25–1 pmol) in immunoblots using a pan-CaMKII–specific antibody.

Because CaMKII displays differing activity states, we evaluated binding under conditions that promoted each configuration. We activated CaMKII with Ca^{2+}/calmodulin (Ca^{2+}/CaM) to release the substrate-binding domain of the kinase from autoinhibitory contacts made in the basal state (25–27) or included Ca^{2+}/CaM and ATP in the binding buffer to allow the transphosphorylation of Thr287 between adjacent kinase monomers within the dodecameric holoenzyme (28). Autophosphorylation sustains kinase activity in the absence of Ca^{2+} elevation and also exposes additional sites for protein-protein interactions (29, 30). Notably, inactive kinase, in its autoinhibited conformation, bound robustly to the channel loop (0.14 ± 0.03 pmol/pmol loop at 20 nM CaMKIIγ_C; $n = 5$) (Figure 1A). This binding was specific to the loop and could not be attributed to the agarose bead or to the N terminus of the glutathione-S-transferase (GST) fusion protein. Moreover, syntide-2, a CaMKII substrate modeled after the CaMKII phosphorylation site of glycogen synthase, could not compete for binding of the inactive kinase at either 50 or 500 μM (Figure 1D), suggesting that the substrate-binding domain of CaMKII is not mediating effector contact. Surprisingly, activation of CaMKII by Ca^{2+} (0.5 mM), CaM (5 mM), and ADP (0.5 mM) had no significant effect on the level of binding (0.12 ± 0.02 pmol/pmol loop; $n = 5$; NS). Nonetheless, the binding of active kinase was effectively competed for by syntide-2. Syntide-2 reduced the binding of active kinase by 38% ± 4% ($n = 4$; $P < 0.05$) and 89% ± 9% ($n = 3$; $P < 0.05$) at 50 μM and 500 μM, respectively (Figure 1D). Taken together these data suggest that the inactive kinase interacts with the α_{1H} II-III loop at a primary contact site that lies outside of its classical substrate-binding domain.

We also examined the binding of catalytically active kinase by replacing ADP with ATP in the activation buffer. ATP (0.5 mM) reduced CaMKII binding by more than 60% to 0.05 ± 0.001 pmol/pmol ($n = 5$), indicating that either CaMKII autophosphorylation or CaMKII phosphorylation of the II-III loop disrupts binding (Figure 1A). Therefore, we examined the binding of CaMKII to a mutated II-III loop in which the major CaMKII phosphorylation

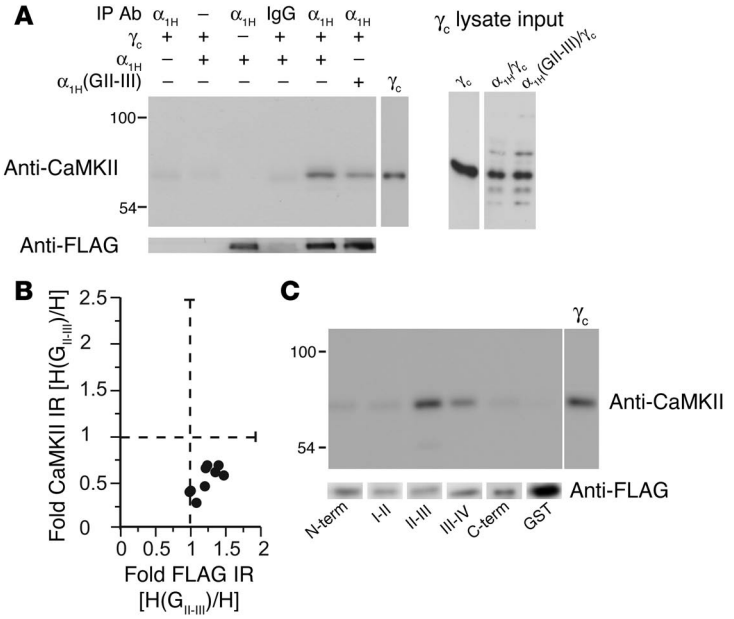

Figure 2

CaMKIIγ_C forms a signaling complex with α_{1H} channels dependent on the II-III loop. (**A**) Immunoblot of channel immunoprecipitates from HEK 293 cells transiently expressing FLAG-tagged α_{1H} wild-type or α_{1H}(GII-III) chimeric channels, most cotransfected with CaMKIIγ_C, using: goat IgG or anti-α_{1H} for the immunoprecipitation, anti-FLAG for verification of channel immunoprecipitation, and anti-CaMKII for detection of CaMKII coassociation. Input lysates show expression level of CaMKIIγ_C with 0.25 pmol purified CaMKIIγ_C standard for comparison. (**B**) An analysis of 9 experiments. Integrated optical band densities of FLAG and CaMKII immunoreactivities (IR) in α_{1H}(GII-III) channel immunoprecipitates expressed relative to immunoreactivities in wild type. (**C**) In vitro binding of purified CaMKIIγ_C (5 pmol/250 μl) to bead-bound channel intracellular domain–GST fusion proteins (2 pmol) of channel intracellular domains: N-terminus (N-term), I-II loop, II-III loop, III-IV loop, C-terminus. Shown are immunoblots of bound kinase detected by anti-CaMKII, with 0.5 pmol standard for comparison. Below is a GST blot for each fusion protein indicating nearly equal loading.

site, Ser1198 (23), was mutated to Ala (Figure 1B). The mutated loop bound similar amounts of inactive CaMKII compared with the wild-type loop (0.15 ± 0.01 pmol/pmol; $n = 5$). Notably, CaMKII activation (Ca^{2+}/CaM + ADP) or autophosphorylation (Ca^{2+}/CaM + ATP) had no significant effect on this interaction (0.15 ± 0.01 pmol/pmol [ADP], 0.13 ± 0.01 pmol/pmol [ATP]; $n = 5$; NS). Thus, Ser1198 substrate phosphorylation appears to initiate the release of the kinase from the channel loop. As expected, we observed no evidence for the binding of inactive, active, or autonomously active CaMKII to the α_{1G} II-III loop fusion protein despite overexposure of our immunoblots (Figure 1C), in agreement with the lack of regulation of α_{1G} channels by CaMKII (22).

To corroborate the above-described findings, we preassembled complexes of inactive CaMKII with wild-type or S1198A-mutated II-III loops and followed the time course of reduction in binding upon activation of the kinase with Ca^{2+}/CaM and ATP/[γ-^{32}P]ATP at 4°C to slow enzymatic activity. Kinase preassociated with the wild-type loop (Figure 1E) was released with a time course ($T_{1/2}$ = 2.1 minutes, for 0–5 minutes, where $T_{1/2}$ represents half-time of dissociation) that approximately paralleled the time course of phosphorylation (Figure 1F) of the loop ($T_{1/2}$ = 2.7 minutes, for 0–5 minutes). At 30°C the rate of debinding was dramatically increased (Figure 1E, inset), consistent with the increased rate of loop phosphorylation (Figure 1F, inset). Mutation of Ser1198 dramatically reduced both phosphate incorporation (73% ± 10%; $n = 3$; Figure 1F) and the dissociation of the kinase (94% ± 4% still bound at 10 minutes; $n = 3$; Figure 1E). Thus, our data show that the interaction of CaMKII with the II-III loop depends on its activity state: inactive kinase forms a stable interaction, whereas the interaction of active kinase is transient. These features are quite distinct from the long-lasting interactions of CaMKII with *N*-methyl-D-aspartic acid (NMDA) receptors (31–35) or ether-a-go-go channels (36, 37) that can keep the active kinase tethered in a catalytically active conformation even in the absence of Ca^{2+} elevation or autophosphorylation.

To determine whether CaMKII interacts with α_{1H} channels in situ, we coexpressed CaMKIIγ_C and FLAG-tagged α_{1H} channels in HEK 293 cells and tested for coimmunoprecipitation. Immunoblotting with a pan-CaMKII–specific antibody often revealed 2 bands of immunoreactivity that coimmunoprecipitated with CaMKIIγ_C-transfected α_{1H} channels: an upper band corresponding to CaMKIIγ_C and a lower band of weaker immunoreactivity, which was less consistently observed and likely to be a truncation product of the expressed kinase construct (Figure 2A). Moreover, CaMKII was not detected in the absence of an immunoprecipitating antibody, in the absence of channel or CaMKII expression, or in the immunoprecipitate of a control immunoglobulin, validating the specificity of the observed coassociation. Because the II-III loop of α_{1H} channels confers regulation to α_{1G} channels that are not modulated by CaMKII, we hypothesized that substitution of the α_{1H} II-III loop with the II-III loop from α_{1G} channels would reduce the amount of CaMKII coimmunoprecipitated. As illustrated in Figure 2A in a representative immunoblot, the chimeric channel immunoprecipitated a fraction of the CaMKII immunoprecipitated by the wild-type α_{1H} channel, despite equivalent levels of CaMKII expression detected in the lysate input. In 3 of 9 experiments where the efficiency of channel immunoprecipitation was equivalent, the α_{1H}(GII-III) chimera immunoprecipitated 33.7% ± 0.5% of the CaMKII immunoreactivity that was immunoprecipitated with the wild-type channel (Figure 2B). Thus, contact sites in the II-III loop play an important role in CaMKII binding to α_{1H} channels in situ. Nonetheless, because one-third of the immunoreactivity was retained by the chimeric channel, we tested for the coassociation of CaMKII with other intracellular channel domains that were expressed as GST fusion proteins. These GST fusion proteins were loaded onto glutathione-sepharose and used in in vitro binding reactions with purified CaMKII. No evidence was obtained for the interaction of CaMKII with the N terminus, the I-II loop, or the C terminus (Figure 2C). However, significant binding to the III-IV loop, representing 10–16% of the binding to the α_{1H} II-III loop, was observed. In principle, CaMKII binding to the III-IV loop can account in part for the residual binding of CaMKII to the α_{1H}(GII-III) chimeric channel.

The identification of α_{1H} channels as a CaMKII-binding partner and the importance of Ser1198 for the modulation of channel gating classify α_{1H} channels as candidate CaMKII substrates.

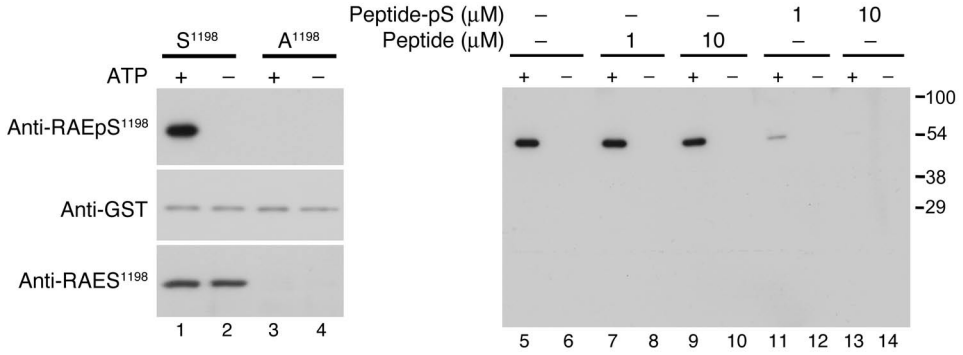

Figure 3

Characterization of phosphomotif-specific antibody targeting RAEpS^{1198}. Immunoblots of in vitro phosphorylation reactions of GST–α_{1H} II-III loop fusion proteins (1 μM) — wild-type (S^{1198}) and mutant (A^{1198}) — catalyzed by 10 nM CaMKIIγ_C (Ca^{2+} [0.5 mM], CaM [2 μM] ± ATP [100 μM]) showing selective recognition of pS^{1198} by anti-RAEpS^{1198} (top row, lanes 1, 5, 7, 9). Below is an anti-GST immunoblot for each fusion, indicating equal loading (middle row, lanes 1–4). Notably, anti-RAES^{1198} recognizes S^{1198} without regard for phosphorylation state (bottom row, lanes 1 and 2). Anti-RAEpS^{1198} preadsorption with phosphopeptide (Peptide-pS, lanes 11–14) but not non-phosphopeptide (Peptide, lanes 7–10) suppressed anti-RAEpS^{1198} immunoreactivity, showing phosphorylation-dependent interaction, confirming phosphomotif specificity.

However, previously there was no direct evidence that Ser1198 was phosphorylated by CaMKII in intact cells. To evaluate Ser1198 phosphorylation in intact cells and tissue, we developed a novel phosphomotif-specific antibody (anti-RAEpS^{1198}) and as a byproduct a motif-specific antibody (anti-RAES^{1198}), enabling us to determine whether α_{1H} channels are authentic kinase substrates. The specificity of the affinity-purified antibody anti-RAEpS^{1198} was evaluated initially using recombinant II-III loop proteins that contained the wild-type sequence or an Ala point mutation at Ser1198. Anti-RAEpS^{1198} recognized only the wild-type II-III loop protein following CaMKII phosphorylation. This phosphorylation-dependent interaction was competed with excess phosphopeptide antigen (pS^{1198} peptide) but not with the non-phosphopeptide (S^{1198} peptide) (Figure 3) and contrasted with anti-RAES^{1198} that recognized the wild-type fusion protein without regard for its phosphorylation state. Moreover, mutation of Ser1198 to Ala precluded recognition by anti-RAEpS^{1198} and anti-RAES^{1198}. Thus, anti-RAEpS^{1198} exhibits appropriate phosphorylation-dependent specificity in vitro.

We generated a HEK 293 cell line stably expressing a mouse leak K^+ channel (mTREK) and FLAG-tagged α_{1H} Ca^{2+} channel (α_{1H}/mTREK) for use in intact cell phosphorylation studies. Ca^{2+} channel currents are robust in these cells, and 6 mM K^+ depolarizes the cell an approximate 20 mV, as indicated in Figure 4A by the rightward shift in the zero current potential of the macroscopic currents, which were measured using a voltage-ramp protocol. Six millimolar K^+ depolarized the membrane potential from –83 ± 4 mV at 2 mM K^+ to –65 ± 3 mV (n = 5). Six millimolar K^+ depolarization also elicited a transient rise in intracellular Ca^{2+} concentration $[Ca^{2+}]_i$, as measured by fluo-4 fluorescence (Figure 4B). This increase in $[Ca^{2+}]_i$ was fully dependent on extracellular Ca^{2+}, dose-dependently attenuated by cellular preincubation with a blocker of LVA Ca^{2+} channel entry (mibefradil at 3 μM and 10 μM), and precluded in cells stably expressing mTREK alone, despite similar changes in membrane potential elicited upon cell depolarization with 6 mM K^+ (–76 ± 3 mV at 2 mM K^+, –52 mV ± 6 mV at 6 mM K^+; n = 6). Taken together these data argue strongly that the measured rise in intracellular Ca^{2+} is mediated by α_{1H} channels.

To investigate whether Ser1198 was phosphorylated in situ, we compared the state of phosphorylation of α_{1H} channels in CaMKIIγ_C-transfected α_{1H}/mTREK cells that had been incubated with 2 mM or 6 mM K^+. To isolate the channel protein, we immunoprecipitated α_{1H} channels from whole-cell lysates using a goat α_{1H}-specific antibody directed against the C-terminal tail of the channel (anti-α_{1H}). Cell stimulation with 6 mM K^+ increased $[Ca^{2+}]_i$ and also increased the phosphorylation state of the α_{1H} channel RAES^{1198} motif in cells expressing CaMKIIγ_C (Figure 4C). The detected increase in RAEpS site immunoreactivity was dependent on Ca^{2+} entry through α_{1H} channels, as it was appropriately attenuated by low calcium (100 μM) or mibefradil (10 μM) preincubation and, as expected, was not observed in the immunoprecipitate of goat IgG. To quantify the increase in phosphorylation state, we evaluated the fold increase in anti-RAEpS immunoreactivity (6 mM K^+/2 mM K^+) and compared it to anti-FLAG immunoreactivity in the immunoprecipitate using a mouse monoclonal FLAG antibody to detect the FLAG-tagged channels. In 8 experiments, K^+-mediated depolarization increased α_{1H} channel RAEpS site immunoreactivity 2- to 4-fold in cells expressing CaMKIIγ_C (230% ± 40%; n = 8; P < 0.001) compared with FLAG immunoreactivity (Figure 4D), which remained unchanged (103% ± 0.03%; n = 8; NS). By contrast, α_{1H} channel RAEpS site immunoreactivity was not increased in the absence of CaMKII transfection (100% ± 0.04%; n = 5; NS). Thus, we conclude that Ser1198 on α_{1H} channels is a bone fide CaMKII phosphorylation site in situ and that this phosphorylation is controlled by membrane depolarization that activates the LVA channel.

Based on our in vitro CaMKII-binding experiments, we hypothesized that the phosphorylation of the RAES motif by CaMKII would disrupt the coassociation of CaMKII and the channel protein. To maximize the degree of kinase autoinhibition and promote docking on the channel, we immunoprecipitated the channel-kinase complex from α_{1H}/mTREK cells that were maintained at 2 mM K^+ and transfected with CaMKIIγ_C. CaMKII in the immunoprecipitated complex was maintained in an inactive conformation or was activated with Ca^{2+}/CaM plus ATP, either alone or following preincubation and maintained incubation with an active (10 μM KN-93) or inactive (10 μM KN-92) CaMKII inhibitor (Figure 5). In the absence of cellular activation, α_{1H} channels formed a complex with the kinase and showed no evidence of RAES site phosphorylation. Activation of the associated kinase in vitro promoted the phosphorylation of the RAES motif and the complete dissociation of the channel-kinase complex, which was prevented by preincubation with the active but not the inactive CaMKII inhibitor. Thus, autoinhibited CaMKII forms a stable complex with the channel that can be fully disrupted by CaMKII activity.

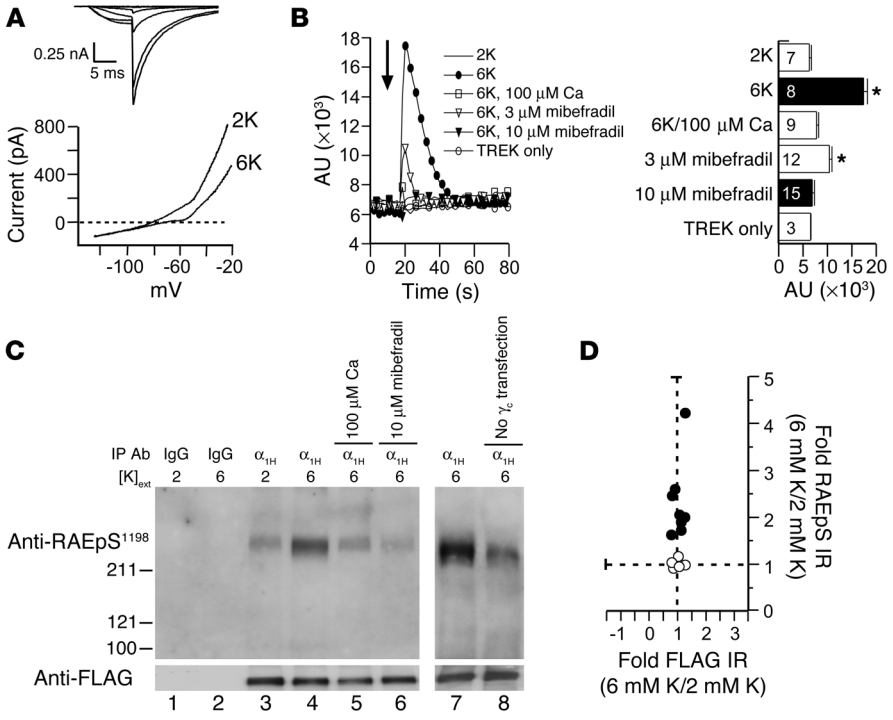

Figure 4

CaMKIIγC-induced phosphorylation of α_{1H} channels in situ. (**A**) Sample currents from α_{1H}/mTREK, transiently expressing CaMKIIγC. Top: α_{1H} tail currents elicited upon repolarization to –60 mV (V_{test} = –50, –30, –10, 0, +10 mV). Bottom: Whole-cell currents elicited by a voltage ramp (–120 to –20 mV). Zero-current potential defines membrane potential (V_m); dashed line highlights V_m change. (**B**) $[Ca^{2+}]_i$ plotted in arbitrary units of fluo-4-fluorescence with time in α_{1H}/mTREK cells (filled circles, open squares, open triangles, filled triangles) or mTREK-only cells (open circles). Six millimolar K^+ (6K) added at 16 seconds. The plain line indicates timed response to 2 mM K^+ challenge in α_{1H}/mTREK cells. Traces are mean response of cells in 3 plate wells. Histograms plot peak (20 seconds) rise in $[Ca^{2+}]_i$ (mean ± SEM; *n* as indicated). Cells were preincubated with 100 μM Ca^{2+} or 10 μM mibefradil 30 minutes prior to 6 mM K^+ challenge and during measurement. **P* < 0.05, 2 mM K^+ versus treatment (ANOVA, Student-Newman-Keuls method). (**C**) Immunoblot of channel-enriched immunoprecipitates (as obtained in Figure 2) from cells challenged with 2 (lanes 1 and 3) or 6 (lanes 2 and 4–8) mM K^+ with (lanes 1–7) or without (lane 8) CaMKIIγC transfection. Channels were immunoprecipitated with a control IgG or anti-α_{1H}. Anti-FLAG verified immunoprecipitation, and anti-RAEpS1198 evaluated phosphorylation. Cells were preincubated with 100 μM Ca^{2+} or 10 μM mibefradil as in **B** (lanes 5–6). (**D**) Analysis of 8 immunoprecipitation experiments. Integrated optical band densities of FLAG and RAEpS1198 immunoreactivities in 6 mM K^+–stimulated samples expressed relative to immunoreactivities in 2 mM K^+ samples in CaMKII-transfected (filled circles) or nontransfected cells (open circles).

To confirm the specificity of the anti-RAEpS1198 antibody in the context of complex interacting cellular proteins, we evaluated the state of phosphorylation of the RAES motif in our α_{1H}/mTREK test system. As illustrated in representative immunoblots (Figure 6A), we detected strong anti-RAEpS1198 diaminobenzidine (DAB) immunostaining in response to 6 mM K^+ depolarization. Notably, this staining was competed with the antigenic peptide (pS1198 peptide) but was not competed with the non-phosphopeptide (S1198 peptide). By contrast anti-RAEpS1198 DAB immunostaining of cells maintained at 2 mM K^+ was weak. Thus, we conclude that anti-RAEpS1198 immunoreactivity reports the phosphorylation state of the RAES motif and immunohistochemistry can be used to determine whether Ser1198 phosphorylation of native LVA channels is also modulated in vivo.

Ang II is a major physiological regulator of aldosterone production from cells of the ZG that robustly express α_{1H} channels (38, 39). Moreover, Ang II activates CaMKII (40), and CaMKII activity is important for sustaining Ang II–stimulated aldosterone secretion (41, 42). Therefore, we harvested adrenal glands from rats following a 30-minute infusion of Ang II (50–200 ng/kg/min) or saline vehicle and compared the phosphorylation of Ser1198 by immunohistochemistry (Figure 6B) to localize the α_{1H} antigen within the ZG and to avoid its dilution with adrenal proteins from other regions. To blunt the fright response and the attendant surge in release of ACTH, itself an aldosterone secretagogue, we administered dexamethasone to the animals 24 hours before study (see Methods). Ang II infusion raised plasma aldosterone concentration 4-fold, from 247 ± 105 to 978 ± 92 pg/ml (mean ± SEM; *n* = 4 and 7 animals, respectively; *P* < 0.004). Following Ang II stimulation, we detected strong anti-RAEpS1198 DAB immunostaining among cells of the ZG that reside directly underneath the capsular envelope (Figure 6B, Ang II/primary Ab). Significantly, this tissue staining was competed with the antigenic pS1198 peptide (Figure 6B, Ang II + pS1198 peptide) but not with the S1198 peptide (Figure 6B, Ang II + S1198 peptide) and replicated the zonal distribution of α_{1H} mRNA detected by in situ hybridization (39). Sections from control tissue (Figure 6B, Control) exhibited consistently weaker DAB immunostaining than those from stimulated tissue (Figure 6B, Ang II). Quantification of anti-RAEpS1198 DAB immunostaining of the ZG (Figure 6C) revealed a 6-fold increase in the staining of Ang II–stimulated tissue (3.9% ± 0.7% to 24.7% ± 3.9% region of interest [ROI]; *P* < 0.006) that was reduced by approximately 60% by preadsorption with an 80-fold molar excess of antigenic phosphopeptide, establishing the α_{1H} channel as a bona fide kinase substrate in vivo.

To determine whether CaMKII was indeed mediating the Ang II–elicited change in S1198 phosphorylation in vivo, we endeavored to blunt CaMKII activation by direct delivery of the water-soluble, cell-permeant CaMKII inhibitor (KN-93) to the subcapsular interstitium of the adrenal cortex. Following uniadrenalectomy and a short surgical recovery period, the remnant adrenal gland was infused in vivo (1 μl/min, 30 minutes) with 5% dextrose (D5W) or D5W containing 100 μM KN-93, prior to and during a systemic infusion of Ang II (50 ng/kg/min, 30 minutes). Blood samples were taken for aldosterone measurement after uniadrenalectomy before the onset and upon the termination of subcapsular infusion to determine the secretory response of the remnant adrenal to Ang II infusion. The remnant gland was harvested, and the phosphorylation state of Ser1198 was compared with that of its preinfused

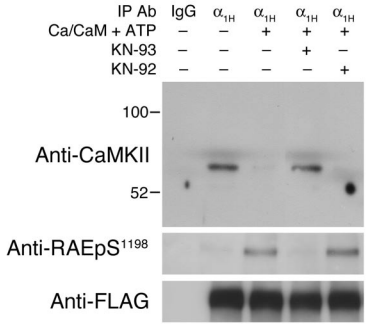

Figure 5

CaMKIIγ_C forms a signaling complex with α_{1H} channels that is disrupted by S^{1198} phosphorylation. Typical immunoblot of channel immunoprecipitates from FLAG- α_{1H}/mTREK double-stable cells incubated at 2 mM K^+ expressing transfected CaMKIIγ_C, using a α_{1H} C terminus–specific antibody for immunoprecipitation and anti-FLAG for verification of channel immunoprecipitation. CaMKII in the immunoprecipitated complex was kept inactive or was activated with Ca^{2+}/CaM + ATP, either alone or following preincubation and maintained incubation with 10 μM of a CaMKII inhibitor, KN-93, or its inactive analog, KN-92. Anti-CaMKII detected CaMKII retained in the immunoprecipitate, and anti-RAEpS1198 assessed the state of S^{1198} phosphorylation.

paired control (Figure 6C). As illustrated in Figure 6C and quantified in the top panel, the direct cortical delivery of KN-93 abrogated the 2-fold increase in $RAEpS^{1198}$ immunostaining of the Ang II–stimulated tissue (20% ± 5.7% ROI [Ang II] versus 3.3% ± 2.7% ROI [Ang II + KN-93]); $n = 3$ each; $P < 0.05$) and concomitantly blunted the aldosterone secretory response of the remnant adrenal to Ang II (1,004 ± 179 pg/ml [Ang II]; 569 ± 40 pg/ml [Ang II + KN-93]); $n = 3$ each; $P < 0.05$). Taken together, our data indicate the participation of a Ca^{2+}/CaM-dependent kinase in the dynamic regulation of Ser1198 by physiological stimuli that activate aldosterone secretion and suggest an important role for channel regulation in the control of aldosterone secretion.

Discussion

Despite decades of research on the regulation of voltage-gated ion channels by protein phosphorylation, few phosphorylation events that alter ion channel activity have been shown to be physiologically modulated in vivo (43–45). This is especially true of the positive feedback regulation of L-type and T-type channels by CaMKII. CaMKII-induced facilitation of L-type Ca^{2+} channels requires active kinase (16, 46, 47), yet the phosphorylation site(s) of functional importance have eluded identification (21, 48).

Previous studies suggested that Ser1198 in α_{1H} channels is required for the potentiation of T-type Ca^{2+} channel current by CaMKII, implicating protein phosphorylation as the mechanism by which CaMKII regulates α_{1H} channels (23). In addition, single-channel experiments using membrane patches excised from native bovine ZG cells demonstrated that CaMKII is contained within the domain of the excised patch, suggesting that channel regulatory elements are locally contained (19). The present study significantly enhances our understanding of the nature of CaMKII–α_{1H} channel interactions and the existence of a CaMKII-channel signaling complex. Our findings provide a biochemical and molecular explanation for how CaMKII modulates LVA Ca^{2+} channels and show that a physiological agonist activates this mechanism to enhance the phosphorylation of α_{1H} channels at Ser1198 in vivo.

We have uncovered what we believe to be a novel mechanism for Ca^{2+}-dependent autoregulation of α_{1H} channels that exploits the changing conformational states of CaMKII. A cycle of autoactivation begins with the docking of inactive CaMKII on the II-III loop of α_{1H} channels under basal conditions (Figure 7A). As a binding partner of the II-III loop, CaMKII is well positioned to sense local Ca^{2+} concentrations that arise from the opening of the LVA channel itself (Figure 7B). The reception of this signal by the kinase induces its activation as well as the transfer of signaling information to Ser1198 as CaMKII shifts its primary interaction with the II-III loop to its catalytic domain as it initiates phosphotransfer (Figure 7C). As is characteristic of interactions between a protein kinase and its substrates (49), phosphorylation of Ser1198 disrupts this association (Figure 7D), dissociating the kinase either to begin a new cycle of autoregulation at another channel or to execute other functions.

These interaction features describe a new paradigm for modulation of ion channel substrates by CaMKII. Inactive kinase does not significantly interact with the cytoplasmic regions of NMDA receptors (31–35), ether-a-go-go channels (36, 37), ryanodine receptors (50), or α_{1C} L-type Ca^{2+} channels (21). Moreover, the recruitment of active kinase to these channels forms long-lasting associations when the kinase is autophosphorylated and new sites of interaction are exposed (T sites). In most instances T site binding produces constitutive kinase activity, keeping the kinase tethered in a catalytically active conformation in the absence of Ca^{2+} elevation or autophosphorylation (31–37).

Notably, our data show that the proposed mechanism for α_{1H} channel modulation by CaMKII is engaged in a model cell by changes in membrane potential that are induced by extracellular K^+ at concentrations that physiologically stimulate ZG cells. Elevation in extracellular K^+ from 2 to 5 mM potentiates the aldosterone secretory response to physiological doses of Ang II (51, 52). Thus, although extracellular K^+ and Ang II can be considered independent regulators of aldosterone production, the physiological potency of these agonists depends on their combined activities and their synergy. Our data provide strong evidence for the operation of this mechanism in the adrenal ZG in response to Ang II signaling in vivo. Thus, Ser1198 in α_{1H} channels is, to our knowledge, the first residue in voltage-gated T-type Ca^{2+} channels shown to be dynamically phosphorylated in vivo. The targeted disruption of docking and/or CaMKII-mediated phosphorylation of α_{1H} channels may offer an alternative therapeutic strategy to that of mineralocorticoid receptor antagonism for limiting the development and progression of cardiovascular damage in heart failure.

Methods

Molecular cloning. A $[His]_6$-FLAG tag was introduced into the wild-type construct GST-H_{II-III} using the mega-primer 5′-AGAAGGTCATCACA-CACAAGTCTAGAGAGAATCTGTATTTCCAAGGCCACCATCACCAT-CACCATGACTACAAGGACGACGATGACAAGAATTCATCGTGACT-GACTGACG-3′ and its reverse compliment in a QuikChange reaction (Stratagene). The GST-H_{II-III} S1198A mutant construct was generated by PCR. All constructs were confirmed by DNA sequencing.

Fluorescence measurement of $[Ca^{2+}]_i$. Cells grown on 96-well plates pretreated (1 hour) with Krebs-HEPES buffer containing 2 mM potassium loaded with fluo-4 AM (30 minutes, 37°C; Invitrogen) were washed prior to experimentation. Fluorescence was monitored with a FlexStation scanning fluorometer (excitation 485 nm, emission 538 nm; Molecular Devices). After 16 seconds baseline scan, signal intensity was monitored (2 minutes, 1.5 Hz) after chal-

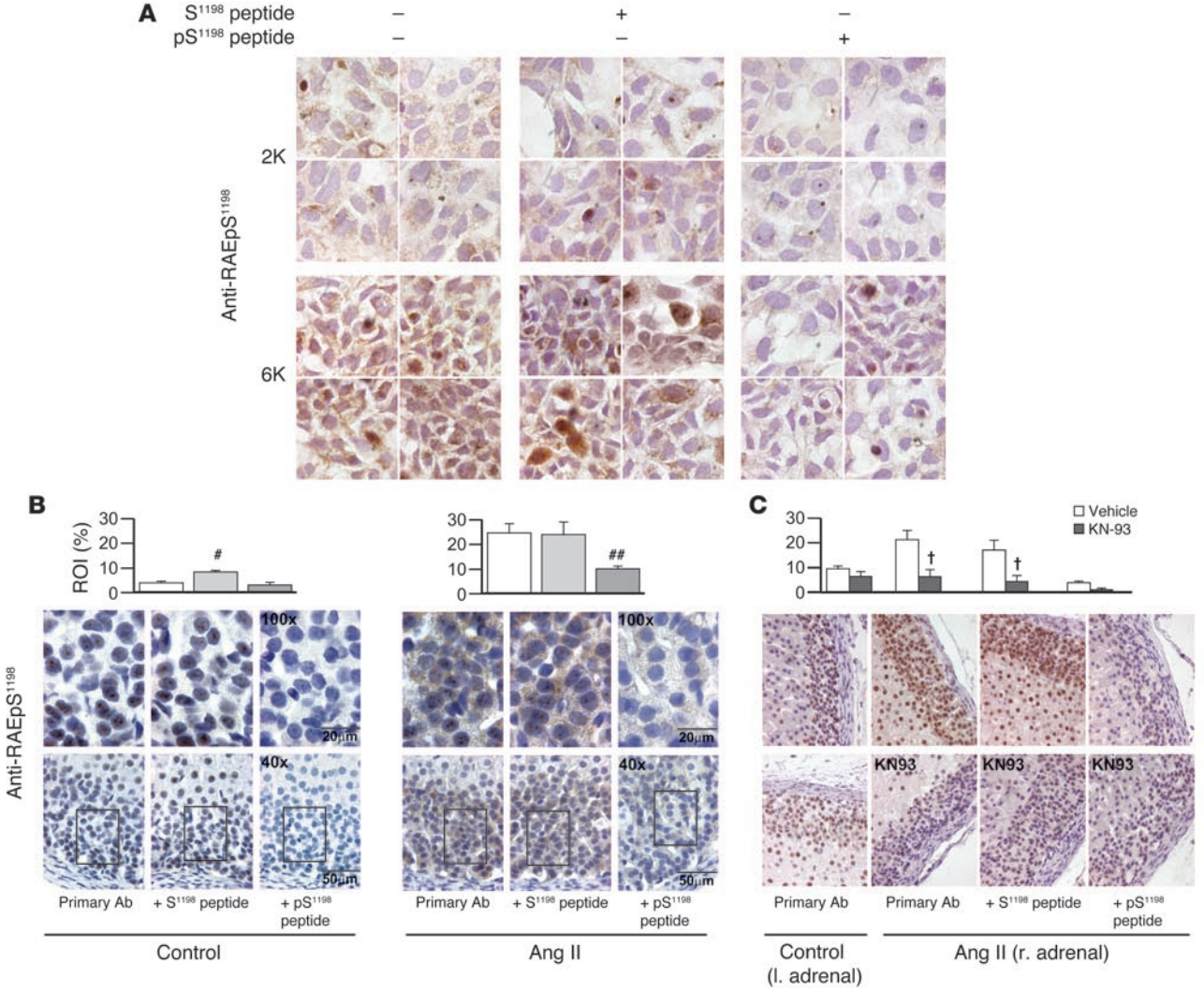

Figure 6

Phosphorylation-state of Ser1198 in α_{1H} channels in situ and in vivo. Immunohistochemical detection of pS^{1198} in: $CaMKII\gamma_C$-transfected α_{1H}/mTREK double-stable cells following 6 mM K^+ depolarization (1 minute) (**A**); thin sections of rat adrenal glands harvested 30 minutes after vehicle or Ang II infusion, 50–200 ng/kg/min (n = 4 and 7 animals, respectively) (**B**); thin sections of rat adrenal glands subcapsularly perfused (1 μl/min) with D5W with or without 100 μM KN-93 30 minutes before and during a 30-minute systemic infusion of Ang II at 50 ng/kg/min in uni-adrenalectomized rats (n = 3 animals each) (**C**). Anti-$RAEpS^{1198}$ immunohistochemistry revealed DAB immunostaining in the subcapsular ZG (**B** and **C**). Note the increase in signal strength after stimulation (**A**–**C**). Signal competed with an 80-fold molar excess of antigenic phosphopeptide, pS^{1198} peptide, but not non-phosphopeptide, S^{1198} peptide, evaluated at either ×40 (**B**, bottom row; and **C**) or ×100 (**B**, top row; and **A**). All samples were counterstained with hematoxylin. Quantification of ZG DAB immunostaining expressed as percent of ROI. $^{\#}P < 0.05$, control S^{1198} peptide versus antibody alone. $^{\#\#}P < 0.05$, stimulated pS^{1198} peptide versus antibody alone (ANOVA on ranks, Student-Newman-Keuls method). $^{\dagger}P < 0.05$, KN-93 versus vehicle, infused using the primary antibody alone or with pS^{1198} peptide preadsorption (ANOVA, Student-Newman-Keuls method).

lenge with 2 or 6 mM K^+. When used, the indicated concentration of mibefradil or 100 μM calcium was present at baseline and during potassium challenge.

Expression and purification of recombinant fusion proteins. Full-length α_{1H} and α_{1G} II-III loop proteins included an N-terminal GST and a C-terminal $[His]_6$-FLAG tag, enabling tandem affinity purification of full-length protein. Transformed bacteria were grown (37°C, OD_{600} 0.4) before induction with isopropyl-β-D-thiogalactopyranoside (IPTG; 0.5 mM, 16 hours, 20°C) and mechanically lysed in PBS. Cleared lysate was affinity purified on Ni-NTA Agarose (QIAGEN) with 6 M urea, refolded overnight using a urea gradient (6 to 0 M), and eluted with 300 mM imidazole.

CaMKII binding and phosphorylation of H_{II-III}. Ni-NTA–purified fusions (GST-H_{II-III}-His-FLAG, GST-G_{II-III}-His-FLAG, or GST-H_{II-III}-RAEA-His-FLAG) were bound to Glutathione Sepharose 4B (Amersham Biosciences; GE Healthcare) beads for 2 hours at 4°C to achieve a final bead loading of 2 pmol of channel loop per sample. Prebound loop was incubated with 5 pmol purified $CaMKII\gamma_C$ at pH 7.5 under basal (100 mM NaCl, 10 mM $MgCl_2$, 0.1% Triton, 50 mM HEPES, 1 mM DTT) or kinase-activating conditions (with 0.5 mM Ca^{2+}, 5 μM CaM, 100 μM ATP, or 100 μM ADP) at 4°C for 8 hours, at which steady-state binding was achieved. Beads equivalently loaded with GST alone served as negative controls. Protein-bound beads were transferred to a Wizard PCR mini-column to facilitate rapid washing with minimal bead loss, washed with PBS, eluted with hot 2× SDS-PAGE loading buffer following 60 seconds high-heat microwave treatment, and recovered by centrifugation (53). Coassociating kinase was immunodetected

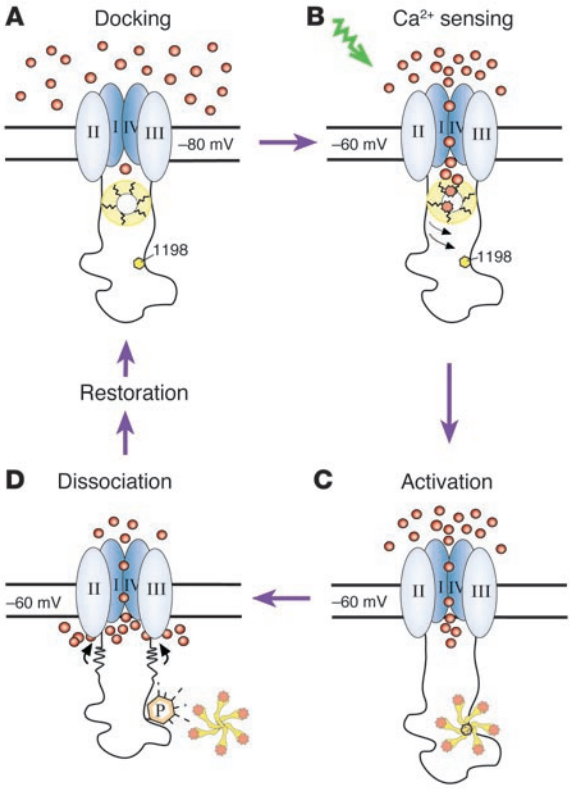

Figure 7
Four-stage mechanistic model of CaMKII and α_{1H} channel interactions. (**A**) Inactive CaMKII docks on the II-III loop of α_{1H} Ca^{2+} channels poised to sense Ca^{2+} influx. (**B**) Depolarization-mediated Ca^{2+} influx elicits a local rise in Ca^{2+} and activates CaMKII. (**C**) Activated CaMKII migrates to S1198 for phosphotransfer. (**D**) CaMKII phosphorylates S^{1198}, provoking further Ca^{2+} influx, and then dissociates. Membrane potential is restored, and the cycle begins anew.

with CaMKII antibody (RU16; a gift of P. Greengard, Rockefeller University, New York, New York, USA) and quantified with recombinant CaMKII standards (0.125–1 pmol) from scanned immunoblots. Equal loading of GST fusion proteins was evaluated on duplicate gels using BSA standards (25–200 ng) stained with SYPRO Ruby (Bio-Rad) or SimplyBlue SafeStain (Invitrogen) (sensitivities of detection >10 ng). Variation in GST loading was tolerated only if values fell within the standard curve and within an experiment did not differ by more than 40%. Binding values were corrected for GST loading differences within the tolerated range. Nonspecific GST-loaded bead binding was typically 0.017 ± 0.012 pmol/pmol loop independent of CaMKII activity state and was subtracted from the totals. In each experiment, samples were analyzed in duplicate.

Phosphorylation-dissociation assays. Inactive CaMKII was prebound (8 hours, 4°C) to channel loop and then activated with Ca^{2+}, CaM, and ATP (4°C). Residual binding was quantified as described above. When concomitantly assessing α_{1H}II-III loop phosphorylation, ^{32}P-ATP was added and SDS-PAGE–separated radiolabeled loop was excised for liquid scintillation counting to determine direct phosphate incorporation.

CaMKII binding to GST-channel loops and termini. PCR fragments corresponding to human α_{1H} (NM_021098) NH_2 terminus (aa 1–99), I-II loop (aa 419–788), II-III loop (aa 1019–1293), III-IV loop (aa 1556–1616), and COOH terminus (aa 1862–2353) were cloned into pGEX-2T and fusions expressed as described above. Glutathione-sepharose beads were preblocked with untransfected HEK cell lysates (1 hour, 4°C) and washed with PBS. Fusion proteins were loaded onto preblocked beads from clarified bacterial lysates containing PBS, 1% Triton X-100, 1 mM PMSF (2 hours, 4°C), achieving a 2-pmol final loading to be used in the CaMKIIγ_C binding assay described above.

Generation and characterization of RAEpS antibody. A phosphomotif-specific antibody recognizing Ser1198 phosphorylation on α_{1H} II-III loop was generated by BioSource, Invitrogen. Rabbits were immunized with acetylated phosphopeptide Ac-LRRAE(pS)LDPC-amide, corresponding to residues 1193–1201 (human α_{1H}). Relevant antisera were purified on non–phosphopeptide–conjugated sepharose to remove non-phosphomotif–specific antibodies, generating anti-$RAES^{1198}$, and the flow-through further purified on a phosphopeptide-affinity resin to select for anti-$RAEpS^{1198}$. Phosphorylation reactions (in mM: 0.5 Ca^{2+}, 0.002 CaM, 10 MgCl, 1 DTT, 45 HEPES, pH 7.5, with or without 0.04 ATP; 37°C, 30 minutes) using purified CaMKIIγ_C (10 nM) and GST–H_{II-III}-His-FLAG and GST-H_{II-III}-RAEA-His-FLAG loop fusions (1 μM) were used to evaluate phosphomotif specificity (32). Products separated on 10% SDS-PAGE and transferred to PVDF were immunoblotted with anti-$RAEpS^{1198}$ (0.04 μg/ml) or anti-$RAES^{1198}$ (0.1 μg/ml). Specificity was assessed by preadsorbing antibody with 1 or 10 μM phospho or non-phosphopeptide for 1 hour.

Immunoprecipitation. HEK 293 or α_{1H}/mTREK double-stables were transfected (48 hours) (Lipofectamine 2000; Invitrogen) with CaMKIIγ_C, and α_{1H} or α_{1H}(GII-III) where appropriate. When stimulated (Figure 4), cells were pretreated (1 hour) with Krebs-HEPES buffer (2 mM K), before 6 mM K^+ (final) or 2 mM K^+ (final, control) challenge (1 minute, 37°C). Termination was initiated by snap-freezing on dry-ice/methanol. Frozen cells were solubilized (in mM: 300 NaCl, 50 Tris HCl, pH 7.5, protease and phosphatase inhibitors [0.025 leupeptin, 0.025 aprotinin, 20 β-glycerol-phosphate, 0.0005 microcystin, 10 pyrophosphate, 0.0001 vanadate], and 0.5% Triton X-100 [1 hour, 4°C]) and centrifuged, and supernatant was precleared with protein G–sepharose. Four micrograms each of anti-α_{1H} antibody or goat IgG (Santa Cruz Biotechnology Inc.) was incubated with 2 mg precleared lysate (2 hours, 4°C), before incubation with protein G (1 hour, 4°C). After sequential bead washing (low-salt buffer: 10 mM Tris-HCl, pH 7.5, 0.2% NP-40, 10 mM EDTA, 150 mM NaCl; high-salt buffer: as above with 500 mM NaCl; and final buffer: 5 mM Tris-HCl, pH 7.5), immunoprecipitated proteins were eluted at 80°C with 2× SDS sample buffer, resolved by 4–15% SDS-PAGE, and analyzed by immunoblot using anti-FLAG (Sigma-Aldrich) and anti-CaMKII (RU-16; P. Greengard).

Electrophysiology. Voltage commands were applied via an EPC7 patch-clamp amplifier and digitized with Digidata 1322A analog-to-digital converter (Axon Instruments). To record macroscopic currents, cells were held at –50 mV, and membrane currents in response to a hyperpolarizing ramp (–20 to –120 mV) were recorded at a constant interval (0.1 Hz) as described previously (54). The bath solution was (in mM): 140 NaCl, 3 KCl, 2 $MgCl_2$, 2 $CaCl_2$, 10 HEPES, 10 glucose, pH 7.4; the pipette solution: 120 $KMeSO_4$, 4 NaCl, 1 $MgCl_2$, 0.5 $CaCl_2$, 10 HEPES, 10 EGTA, 3 MgATP, 0.3 GTP-Tris, pH 7.2. Ca^{2+} channel tail currents were elicited in response to 15 test depolarizations in 5-mV increments (–60 to +10 mV; 10.4 ms) from a holding potential of –90 mV during repolarization to –60 mV (45 ms), as previously described (23). The bath solution was (in mM): 127 TEA-Cl, 10 $CaCl_2$, 0.5 $MgCl_2$, 10 HEPES, 5 dextrose, 32 sucrose, pH 7.4 (CsOH adjusted); the pipette solution: 115 CsCl, 1 tetrabutylammonium chloride, 1 $MgCl_2$, 5 Mg ATP, 1 LiGTP, 20 HEPES, 0.9 mM $CaCl_2$, 11 BAPTA, pH 7.2 (CsOH adjusted).

Animal surgeries. Animals were pretreated with dexamethasone (i.p.: 0.3–1 mg/kg) 16 and 4 hours before surgery, which inhibited any ACTH-mediated fright response induced by animal handling and anesthesia administration. Female rats (~220 g) were treated (30 minutes) by jugular infusion of either an isotonic D5W solution or one containing 50–200 ng/kg/min

Ang II. Plasma aldosterone levels were assayed before and after infusion (Aldosterone Coat-a-Count; Diagnostic Products Corp.). Following infusion, rats were perfused transcardially with fresh 4% paraformaldehyde (PFA) and the adrenals harvested.

Uniadrenalectomy studies. Following anesthesia, the left adrenal vein and artery were ligated for gland removal into 4% PFA (control), the right femoral vein cannulated and prepared for infusion, and the right femoral artery cannulated to facilitate mean arterial blood pressure recording. In addition, a PE-10 catheter was placed in the subcapsular area of the remnant adrenal gland, secured using Vetbond (3M Tissue Adhesive; 3M Animal Care Products), and infused in vivo (1 μl/min, 30 minutes) with D5W alone or containing 100 μM KN-93, prior to and during a systemic infusion of Ang II (50 ng/kg/min, 30 minutes). To harvest adrenals, rats were perfused transcardially with fresh 4% PFA. All animal experiments were performed in accordance with NIH policies and approved by the University of Virginia Medical Center Institutional Animal Care and Use Committee.

Immunohistochemistry. Harvested adrenals were dehydrated and paraffin embedded before sectioning (5 μm) onto slides. Sections were deparaffinized, rehydrated, and quenched with H_2O_2. The tissue antigenic sites were unmasked (unmasking reagent; Vector Laboratories) and slides washed extensively in PBS with porcine gelatin (PBS/PG). Sections preblocked with 10% goat serum in PBS/PG were incubated sequentially with: anti-RAEpS^{1198} (4°C, 16 hours; 1:800) alone or preadsorbed with phosphopeptide (pS^{1198} peptide) or non-phosphopeptide (S^{1198} peptide) at 80-fold excess, biotinylated goat anti-rabbit secondary antibody (room temperature, 1 hour; Vector Laboratories), and avidin-biotin-HRP complex (room temperature, 0.5 hours; VECTASTAIN Elite ABC kit; Vector Laboratories). The HRP complex was detected using DAB (Dako), slides counterstained with hematoxylin (Richard-Allan Scientific), and dehydrated in ethanol then xylene before coverslipping in Krystalon (EM Science Harleco) (55). Images were obtained using QImaging Retiga 1300C digital camera fitted to a Zeiss microscope and processed using IPLab (Scanalytics).

Four quadrants of each section were photographed and the ZG area selected using IPLab's polygon ROI for analysis of percent DAB staining. IPLab software version 3.65 (BD) was scripted to identify pixels with Hue, Saturation, and Value (HSV) parameters appropriate to define brown hues of varying intensity.

Immunocytochemistry. α_{1H}/mTREK cells grown on poly-lysine–coated 12-well HTC super-cured slides (Cel-Line) were pretreated (1 hour) with standard Krebs-HEPES buffer (2 mM K^+) stimulated (1 minute, 37°C) with 6 mM K^+ final or 2 mM K^+ (control), immediately fixed with 4% PFA, and permeabilized with 1% Triton X-100.

Statistics. Multiple comparisons were evaluated using ANOVA with Student-Newman-Keuls method for post-hoc testing or an unpaired 2-tailed Student's *t* test when appropriate (SigmaStat; Jandel Scientific, SPSS). *P* values less than 0.05 were considered statistically significant.

Specialized reagents. A cDNA encoding porcine CaMKIIγ_C, a generous gift from C.M. Schworer and H.A. Singer (Albany Medical College, Albany, New York, USA), was cloned into PVL1392 to generate recombinant baculovirus. Sf9 insect cells infected with plaque-purified recombinant baculovirus (MOI = 10) were harvested after 72 hours. The protein was purified by ammonium sulfate precipitation followed by affinity chromatography on CaM-agarose. CaMKIIγ_C was dialyzed against 50 mM HEPES pH 7.5 containing 50% (vol/vol) glycerol, 10% (vol/vol) ethylene glycol, 2.5 mM EDTA, 1 mM DTT and stored (–20°C). Protein purity (>95%) was assessed by Coomassie blue–stained SDS-polyacrylamide gels and expressed a specific activity of 10–20 μmol/min/mg (syntide-2 substrate, 20 μM) (56).

Acknowledgments

We acknowledge support from NIH grants (HL36977 to P.Q. Barrett and MH63232 to R.J. Colbran) and American Heart Association MidAtlantic-Affiliate postdoctoral fellowships to J. Yao and L.A. Davies.

Received for publication January 13, 2006, and accepted in revised form June 20, 2006.

Address correspondence to: Paula Q. Barrett, Department of Pharmacology, University of Virginia School of Medicine, 1300 Jefferson Park Avenue, Charlottesville, Virginia 22908, USA. Phone: (434) 924-5454; Fax: (434) 982-3878; E-mail: pqb4b@virginia.edu.

J.D. Howard's present address is: Department of Pharmacology and Molecular Sciences, Johns Hopkins University School of Medicine, Baltimore, Maryland, USA.

P.J. Welsby's present address is: Department of Physiology, Trinity College, Dublin, Ireland.

1. Pogwizd, S.M., and Bers, D.M. 2004. Cellular basis of triggered arrhythmias in heart failure. *Trends Cardiovasc. Med.* **14**:61–66.
2. Anderson, M.E. 2005. The fire from within: the biggest Ca channel erupts and dribbles. *Circ. Res.* **97**:1213–1215.
3. Bers, D.M., Eisner, D.A., and Valdivia, H.H. 2003. Sarcoplasmic reticulum Ca2+ and heart failure: roles of diastolic leak and Ca2+ transport. *Circ. Res.* **93**:487–490.
4. Pogwizd, S.M., Schlotthauer, K., Li, L., Yuan, W., and Bers, D.M. 2001. Arrhythmogenesis and contractile dysfunction in heart failure: roles of sodium-calcium exchange, inward rectifier potassium current, and residual beta-adrenergic responsiveness. *Circ. Res.* **88**:1159–1167.
5. Schroder, F., et al. 1998. Increased availability and open probability of single L-type calcium channels from failing compared with nonfailing human ventricle. *Circulation.* **98**:969–976.
6. Perrier, E., et al. 2004. Mineralocorticoid receptor antagonism prevents the electrical remodeling that precedes cellular hypertrophy after myocardial infarction. *Circulation.* **110**:776–783.
7. Perrier, R., et al. 2005. A direct relationship between plasma aldosterone and cardiac L-type Ca2+ current in mice. *J. Physiol. (Lond.).* **569**:153–162.
8. Brilla, C.G., and Weber, K.T. 1992. Mineralocorticoid excess, dietary sodium, and myocardial fibrosis. *J. Lab. Clin. Med.* **120**:893–901.
9. Funder, J.W. 1995. Steroids, hypertension and cardiac fibrosis. *Blood Press. Suppl.* **2**:39–42.
10. Pitt, B., Stier, C.T., Jr., and Rajagopalan, S. 2003. Mineralocorticoid receptor blockade: new insights into the mechanism of action in patients with cardiovascular disease. *J. Renin Angiotensin Aldosterone Syst.* **4**:164–168.
11. Quinn, S.J., and Williams, G.H. 1988. Regulation of aldosterone secretion. *Annu. Rev. Physiol.* **50**:409–426.
12. Spat, A., and Hunyady, L. 2004. Control of aldosterone secretion: a model for convergence in cellular signaling pathways. *Physiol. Rev.* **84**:489–539.
13. Barrett, P.Q., Isales, C.M., Bollag, W.B., and McCarthy, R.T. 1991. Ca2+ channels and aldosterone secretion: modulation by K+ and atrial natriuretic peptide. *Am. J. Physiol.* **261**:F706–F719.
14. Rossier, M.F., Burnay, M.M., Vallotton, M.B., and Capponi, A.M. 1996. Distinct functions of T- and L-type calcium channels during activation of bovine adrenal glomerulosa cells. *Endocrinology.* **137**:4817–4826.
15. Rossier, M.F., et al. 1996. Sources and sites of action of calcium in the regulation of aldosterone biosynthesis. *Endocr. Res.* **22**:579–588.
16. Dzhura, I., Wu, Y., Colbran, R.J., Balser, J.R., and Anderson, M.E. 2000. Calmodulin kinase determines calcium-dependent facilitation of L-type calcium channels. *Nat. Cell Biol.* **2**:173–177.
17. Hoch, B., Meyer, R., Hetzer, R., Krause, E.G., and Karczewski, P. 1999. Identification and expression of delta-isoforms of the multifunctional Ca2+/calmodulin-dependent protein kinase in failing and nonfailing human myocardium. *Circ. Res.* **84**:713–721.
18. Zhang, R., et al. 2005. Calmodulin kinase II inhibition protects against structural heart disease. *Nat. Med.* **11**:409–417.
19. Lu, H.K., Fern, R.J., Nee, J.J., and Barrett, P.Q. 1994. Ca(2+)-dependent activation of T-type Ca2+ channels by calmodulin-dependent protein kinase II. *Am. J. Physiol.* **267**:F183–F189.
20. Dzhura, I., et al. 2002. Cytoskeletal disrupting agents prevent calmodulin kinase, IQ domain and voltage-dependent facilitation of L-type Ca2+ channels [erratum 2003, 546:955]. *J. Physiol.* **545**:399–406.
21. Hudmon, A., et al. 2005. CaMKII tethers to L-type

Ca2+ channels, establishing a local and dedicated integrator of Ca signals for facilitation. *J. Cell Biol.* **171**:537–547.
22. Wolfe, J.T., Wang, H., Perez-Reyes, E., and Barrett, P.Q. 2002. Stimulation of recombinant Ca(v)3.2, T-type, Ca(2+) channel currents by CaMKIIgamma(C). *J. Physiol.* **538**:343–355.
23. Welsby, P.J., et al. 2003. A mechanism for the direct regulation of T-type calcium channels by Ca2+/calmodulin-dependent kinase II. *J. Neurosci.* **23**:10116–10121.
24. Perez-Reyes, E. 1999. Three for T: molecular analysis of the low voltage-activated calcium channel family. *Cell. Mol. Life Sci.* **56**:660–669.
25. Smith, M.K., Colbran, R.J., Brickey, D.A., and Soderling, T.R. 1992. Functional determinants in the autoinhibitory domain of calcium/calmodulin-dependent protein kinase II. Role of His282 and multiple basic residues. *J. Biol. Chem.* **267**:1761–1768.
26. Cruzalegui, F.H., et al. 1992. Regulation of intrasteric inhibition of the multifunctional calcium/calmodulin-dependent protein kinase. *Proc. Natl. Acad. Sci. U. S. A.* **89**:12127–12131.
27. Yang, E., and Schulman, H. 1999. Structural examination of autoregulation of multifunctional calcium/calmodulin-dependent protein kinase II. *J. Biol. Chem.* **274**:26199–26208.
28. Hanson, P.I., Meyer, T., Stryer, L., and Schulman, H. 1994. Dual role of calmodulin in autophosphorylation of multifunctional CaM kinase may underlie decoding of calcium signals. *Neuron.* **12**:943–956.
29. Lai, Y., Nairn, A.C., and Greengard, P. 1986. Autophosphorylation reversibly regulates the Ca2+/calmodulin-dependence of Ca2+/calmodulin-dependent protein kinase II. *Proc. Natl. Acad. Sci. U. S. A.* **83**:4253–4257.
30. Schworer, C.M., Colbran, R.J., and Soderling, T.R. 1986. Reversible generation of a Ca2+-independent form of Ca2+(calmodulin)-dependent protein kinase II by an autophosphorylation mechanism. *J. Biol. Chem.* **261**:8581–8584.
31. Strack, S., and Colbran, R.J. 1998. Autophosphorylation-dependent targeting of calcium/calmodulin-dependent protein kinase II by the NR2B subunit of the N-methyl-D-aspartate receptor. *J. Biol. Chem.* **273**:20689–20692.
32. Strack, S., McNeill, R.B., and Colbran, R.J. 2000. Mechanism and regulation of calcium/calmodulin-dependent protein kinase II targeting to the NR2B subunit of the N-methyl-D-aspartate receptor. *J. Biol. Chem.* **275**:23798–23806.
33. Bayer, K.U., De Koninck, P., Leonard, A.S., Hell, J.W., and Schulman, H. 2001. Interaction with the NMDA receptor locks CaMKII in an active conformation. *Nature.* **411**:801–805.
34. Leonard, A.S., et al. 2002. Regulation of calcium/calmodulin-dependent protein kinase II docking to N-methyl-D-aspartate receptors by calcium/calmodulin and alpha-actinin. *J. Biol. Chem.* **277**:48441–48448.
35. Schulman, H. 2004. Activity-dependent regulation of calcium/calmodulin-dependent protein kinase II localization. *J. Neurosci.* **24**:8399–8403.
36. Wang, Z., Wilson, G.F., and Griffith, L.C. 2002. Calcium/calmodulin-dependent protein kinase II phosphorylates and regulates the Drosophila eag potassium channel. *J. Biol. Chem.* **277**:24022–24029.
37. Sun, X.X., Hodge, J.J., Zhou, Y., Nguyen, M., and Griffith, L.C. 2004. The eag potassium channel binds and locally activates calcium/calmodulin-dependent protein kinase II. *J. Biol. Chem.* **279**:10206–10214.
38. Cohen, C.J., McCarthy, R.T., Barrett, P.Q., and Rasmussen, H. 1988. Ca channels in adrenal glomerulosa cells: K+ and angiotensin II increase T-type Ca channel current. *Proc. Natl. Acad. Sci. U. S. A.* **85**:2412–2416.
39. Schrier, A.D., Wang, H., Talley, E.M., Perez-Reyes, E., and Barrett, P.Q. 2001. alpha1H T-type Ca2+ channel is the predominant subtype expressed in bovine and rat zona glomerulosa. *Am. J. Physiol. Cell Physiol.* **280**:C265–C272.
40. Fern, R.J., et al. 1995. Ca2+/calmodulin-dependent protein kinase II activation and regulation of adrenal glomerulosa Ca2+ signaling. *Am. J. Physiol.* **269**:F751–F760.
41. Pezzi, V., Clark, B.J., Ando, S., Stocco, D.M., and Rainey, W.E. 1996. Role of calmodulin-dependent protein kinase II in the acute stimulation of aldosterone production. *J. Steroid Biochem. Mol. Biol.* **58**:417–424.
42. Pezzi, V., Clyne, C.D., Ando, S., Mathis, J.M., and Rainey, W.E. 1997. Ca(2+)-regulated expression of aldosterone synthase is mediated by calmodulin and calmodulin-dependent protein kinases. *Endocrinology.* **138**:835–838.
43. Yang, L., et al. 2005. Ser1928 is a common site for Cav1.2 phosphorylation by protein kinase C isoforms. *J. Biol. Chem.* **280**:207–214.
44. Davare, M.A., and Hell, J.W. 2003. Increased phosphorylation of the neuronal L-type Ca(2+) channel Ca(v)1.2 during aging. *Proc. Natl. Acad. Sci. U. S. A.* **100**:16018–16023.
45. Haase, H., Bartel, S., Karczewski, P., Morano, I., and Krause, E.G. 1996. In-vivo phosphorylation of the cardiac L-type calcium channel beta-subunit in response to catecholamines. *Mol. Cell. Biochem.* **163–164**:99–106.
46. Yuan, W., and Bers, D.M. 1994. Ca-dependent facilitation of cardiac Ca current is due to Ca-calmodulin-dependent protein kinase. *Am. J. Physiol.* **267**:H982–H993.
47. Anderson, M.E., Braun, A.P., Schulman, H., and Premack, B.A. 1994. Multifunctional Ca2+/calmodulin-dependent protein kinase mediates Ca(2+)-induced enhancement of the L-type Ca2+ current in rabbit ventricular myocytes. *Circ. Res.* **75**:854–861.
48. Abiria, S.A., et al. 2006. Ca2+/calmodulin dependent protein kinase II (CaMKII) interacts with L-type calcium channel (LTCC) beta subunits. Abstract presented at the 35th Annual Meeting of the Society for Neuroscience. November 12–16. Washington, DC, USA. 2005 Abstract Viewer/Itinerary Planner. Program no. 726.713.
49. Buck, E., and Iyengar, R. 2003. Organization and functions of interacting domains for signaling by protein-protein interactions. *Science STKE.* **209**:re14.
50. Ai, X., Curran, J.W., Shannon, T.R., Bers, D.M., and Pogwizd, S.M. 2005. Ca2+/calmodulin-dependent protein kinase modulates cardiac ryanodine receptor phosphorylation and sarcoplasmic reticulum Ca2+ leak in heart failure. *Circ. Res.* **97**:1314–1322.
51. Chen, X.L., Bayliss, D.A., Fern, R.J., and Barrett, P.Q. 1999. A role for T-type Ca2+ channels in the synergistic control of aldosterone production by ANG II and K+. *Am. J. Physiol.* **276**:F674–F683.
52. Spat, A. 2004. Glomerulosa cell — a unique sensor of extracellular K+ concentration. *Mol. Cell. Endocrinol.* **217**:23–26.
53. Wu, J., Kleiner, U., and Brautigan, D.L. 1996. Protein phosphatase type-1 and glycogen bind to a domain in the skeletal muscle regulatory subunit containing conserved hydrophobic sequence motif. *Biochemistry.* **35**:13858–13864.
54. Washburn, C.P., Sirois, J.E., Talley, E.M., Guyenet, P.G., and Bayliss, D.A. 2002. Serotonergic raphe neurons express TASK channel transcripts and a TASK-like pH- and halothane-sensitive K+ conductance. *J Neurosci.* **22**:1256–1265.
55. Day, Y.J., et al. 2005. A2A adenosine receptors on bone marrow-derived cells protect liver from ischemia-reperfusion injury. *J. Immunol.* **174**:5040–5046.
56. Colbran, R.J. 1993. Inactivation of Ca2+/calmodulin-dependent protein kinase II by basal autophosphorylation. *J. Biol. Chem.* **268**:7163–7170.